International Dairy Journal 164 (2025) 106187

Contents lists available at ScienceDirect

International Dairy Journal

journal homepage: www.elsevier.com/locate/idairyj

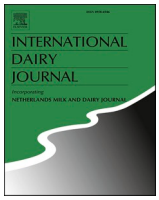

Research paper

Effects of whey protein treatment in an *in vitro* intestinal cell model following oxidative stress or inflammatory challenge

Esther Willems [a], Ajitpal Purba [b], Matthew S. Savoian [c], Charles Hefer [a], Evelyne Maes [a], Dulantha Ulluwishewa [b,*]

[a] AgResearch, Smart Foods & Bioproducts, Tuhiraki, Lincoln, New Zealand
[b] AgResearch, Smart Foods & Bioproducts, Joint Food Science Facility, Palmerston North, New Zealand
[c] School of Natural Sciences, Massey University, Palmerston North, New Zealand

ARTICLE INFO

Keywords:
Tight junctions
Reactive oxygen species
Data-independent acquisition
Intracellular proteome

ABSTRACT

Bovine milk whey proteins with an isoelectric point >6.8 ('whey') have demonstrated anti-inflammatory and antioxidant properties. In the present study, pre-treatment of human intestinal cells (Caco-2) with whey mitigated intracellular reactive oxygen species produced in response to the pro-oxidant 2,2′-azobis (2-methylpropionamide)-dihydrochloride (AAPH). The mitigating effect was dose-dependent, and persisted when whey was removed prior to the addition of AAPH. Whey treatment also improved transepithelial electrical resistance (TEER), but returned to untreated-control levels upon removal of whey. Hence, whey can lead to cellular adaptations that aid intestinal function, but can exert additional properties while in contact with cells. Confocal imaging indicated that the previously observed TEER improvements in inflammatory-challenged Caco-2 monolayers were not due to the localisation of occludin or zonula occludens-1 tight junction proteins. However, proteomics analysis indicated a role for other tight junction proteins and provided insights into cellular adaptations that occur in response to whey pre-treatment.

1. Introduction

In addition to its role in food digestion and nutrient absorption, the human intestine functions as a selectively permeable barrier (Bischoff et al., 2014). While the intestinal barrier is a complex multilayer system, its main physical component is the intestinal epithelium. This is a single layer of intestinal epithelial cells separating the intestinal lumen from the internal milieu. The spaces between the epithelial cells are sealed by tight junction (TJ) protein components that restrict the paracellular passage of toxins, pathogens, and other unwanted luminal antigens across the epithelium (Suzuki, 2013). However, inflammatory mediators such as cytokines and reactive oxygen species (ROS) can disrupt the epithelial barrier function (Rao, 2008). When barrier function is compromised, abnormal antigen exposure can result in disruption of the balance between tolerance and immune activation, which if not managed, can lead to intestinal disorders. In line with this, several intestinal disorders (such as coeliac disease, inflammatory bowel disease, and irritable bowel syndrome) are characterised by barrier dysfunction, and restoring the barrier function has been shown to have beneficial effects (Stolfi, Maresca, Monteleone, & Laudisi, 2022).

Oxidative stress is an imbalance between the production and elimination of ROS, where excessive elevation of ROS can be caused by various environmental factors including pollutants, radiation, and lifestyle. Oxidative stress can disrupt the intestinal barrier function by modulating the activity of signalling molecules and pathways involved in TJ regulation (Basuroy et al., 2003; Rao, 2008; Samak et al., 2016). Excessive ROS can also lead to the activation of the immune system, causing inflammation which exacerbates barrier dysfunction (Y. Wang, Chen, Zhang, Lu, & Chen, 2020). This infiltration of the intestine by immune cells such as macrophages and neutrophils, stimulates further production of ROS. Therefore, dietary supplements that can serve as natural antioxidants have attracted attention as a method to maintain ROS balance and hence proper barrier function. In particular, there is a strong interest in studying and identifying bioactive components in milk that can be used to produce functional foods (Giromini, Cheli, Rebucci, & Baldi, 2019).

Lactoferrin, a minor protein that occurs in the whey fraction of bovine milk, has antioxidative properties and interacts synergistically

* Corresponding author.
E-mail address: dulantha.ulluwishewa@agresearch.co.nz (D. Ulluwishewa).

https://doi.org/10.1016/j.idairyj.2025.106187
Received 1 August 2024; Received in revised form 14 January 2025; Accepted 15 January 2025
Available online 17 January 2025

with other minor whey proteins such as immunoglobulins and lactoperoxidase (Farnaud & Evans, 2003; Graikini et al., 2024; Ostertag & Hinrichs, 2023). Separation of whey proteins based on an isoelectric point (pI) of 6.8 leads to the increased concentration of several of these minor bioactive whey proteins, by eliminating the major whey proteins such as α-lactalbumin (~20 % of whey) and β-lactoglobulin (~50 % of whey) (Abd El-Salam & El-Shibiny, 2017). We recently showed that a commercially available whey ingredient, which contains all bovine milk whey proteins with a pI > 6.8 (henceforth referred to as 'whey' or 'whey protein'), was shown to improve intestinal barrier function in an *in vitro* model of the intestinal epithelium (Ulluwishewa, Mullaney, Adam, Claycomb, & Anderson, 2022). Furthermore, when the epithelium was challenged with tumour necrosis factor α (TNFa) to mimic a "leaky" barrier, whey protein was able to mitigate the observed barrier dysfunction.

In the present study we sought to further examine how whey protein can protect against inflammation and oxidative stress induced barrier dysfunction *in vitro*. Our hypotheses were that (i) the previously observed protective effects of whey were caused by the re-localisation of TJ proteins occludin and Zonula occludens (ZO)-1, (ii) pre-treatment of intestinal epithelial cells with whey is sufficient to protect against TNFa-induced barrier dysfunction, and (iii) whey protein can protect cells against the effects of oxidative-stress. First, using differentiated Caco-2 monolayers as a model of the intestinal barrier (Hidalgo, Raub, & Borchardt, 1989; Pinto, Robine, & Appay, 1983), we investigated the effects of whey and TNFa on localisation of TJ proteins, and epithelial ion permeability. Next, the effects of whey on intracellular ROS production and barrier integrity were assessed following 2,2′-Azobis (2-amidinopropane) dihydrochloride (AAPH)-induced oxidative stress. Finally, the intracellular proteome was assessed by data-independent acquisition (DIA) mass spectrometry analysis to gain mechanistic insights into the antioxidative effects of whey.

2. Materials and methods

2.1. Whey protein powder

The whey protein powder used in this study is commercially available ('IDP®'), and was provided by Quantec Ltd (Hamilton, New Zealand). This product was commercially produced using bovine milk via an industrial process which results in a free-flow beige powder (≥90 % protein) containing all bovine milk whey proteins with pI > 6.8, in approximately the same ratios as found natively in bovine milk. Further details on how the powder was produced are described elsewhere (Ulluwishewa et al., 2022). Many major milk proteins, such as casein, α-lactalbumin, and β-lactoglobulin, are absent in the whey protein powder, which is enriched in minor bioactive whey proteins. The batch of whey protein powder used in this study contained lactoferrin (379 $mg{\cdot}mL^{-1}$), lactoperoxidase (193 $mg{\cdot}mL^{-1}$), lysosomal alpha-mannosidase (0.93 $mg{\cdot}mL^{-1}$), quiescin (3.77 $mg{\cdot}mL^{-1}$), immunoglobulin G1 (86 $mg{\cdot}mL^{-1}$), jacalin-like protein (0.06 $mg{\cdot}mL^{-1}$), angiogenin (16.02 $mg{\cdot}mL^{-1}$), and ribonuclease 4 (16 $mg{\cdot}mL^{-1}$). While these are the only eight proteins made publicly known, over 50 different proteins have been identified in these particular whey fractions (Quantec Ltd., personal communication).

2.2. Caco-2 cell culture

Caco-2 cells (HTP-37) were obtained from the American Type Culture Collection at passage 17, and used in experiments at passages 29–33. Cells were cultured in Minimum Essential Medium (MEM; Thermo Fisher Scientific, Waltham, USA) containing 10 % (v/v) foetal bovine serum (FBS; Moregate BioTech, Hamilton, New Zealand) and 1 % MEM non-essential amino acids (100 × solution; NEAA; Thermo Fisher Scientific, Waltham, USA) at 37 °C in a 5 % CO_2 humidified environment. Cells were routinely maintained in T75 or T175 cell culture flasks (Thermo Fisher Scientific, Waltham, USA), and passaged every ~7 days when cells reached 70–80 % confluence. For experiments, cells were seeded on 6.5 mm Transwells with 0.4 μm pore polyester membrane inserts (Sigma-Aldrich, St. Louis, USA)) at a density of 3×10^5 cells/insert except where otherwise indicated. Cells on Transwell inserts were cultured for 19–21 days with medium changes every 2–3 days, to allow for spontaneous differentiation, prior to treatment. Cell culture treatments were prepared by diluting treatment in MEM containing 1 % (v/v) NEAA unless specified otherwise. The reason for excluding FBS from the treatment medium was in case it interfered with the bioactivity of the treatments. Prior to treatment, cells were allowed to equilibrate for approximately 24 h in MEM containing 1 % (v/v) NEAA to ensure any treatment effects observed were not due to the removal of FBS. Once prepared, stock solutions of treatments were filter-sterilised using a 0.22 μm polyethersulfone membrane, following which the stock solution was diluted to the desired concentration in the appropriate culture medium. During treatment/challenge, cells were incubated at 37 °C in a 5 % CO_2 humidified environment.

2.3. Tight junction barrier morphology assessments

Differentiated Caco-2 monolayers on Transwell inserts were treated with 260 μL of 0 or 1 $mg{\cdot}mL^{-1}$ whey protein. The basal culture medium in the Transwell plate was replaced with 810 μL of MEM containing 10 % (v/v) FBS and 1 % (v/v) NEAA containing either 0 or 100 $ng{\cdot}mL^{-1}$ of TNFa (Thermo Fisher Scientific, Waltham, USA) challenge (three monolayers per treatment-challenge combination). Following 24 h of treatment, Caco-2 monolayers were washed with phosphate-buffered saline (pH 7.2; PBS; Thermo Fisher Scientific, Waltham, USA), fixed in 4 % (w/v) paraformaldehyde (Sigma-Aldrich, St. Louis, USA) for 15 min, and permeabilised in PBS containing 0.2 % (v/v) Triton X-100 (Lab-Chem, Zelienople, USA), 1 % (v/v) normal goat serum (Thermo Fisher Scientific, Waltham, USA), and 0.1 % (w/v) sodium azide (Merck, Burlington, USA). The monolayers were incubated overnight at 4 °C in 1 $\mu g{\cdot}mL^{-1}$ of polyclonal rabbit anti-occludin (Thermo Fisher Scientific, Waltham, USA) and monoclonal mouse anti-ZO-1 (Thermo Fisher Scientific, Waltham, USA), washed five times in PBS containing 0.1 % (v/v) Triton X-100 to remove non-specific binding, and incubated for 2 h at room temperature in 8 μg/mL of Alexa Fluor 555 conjugated goat anti-rabbit IgG (Thermo Fisher Scientific, Waltham, USA), and Alexa Fluor 488 conjugated goat anti-mouse IgG (Thermo Fisher Scientific, Waltham, USA). The monolayers were washed five times in PBS containing 0.1 % (v/v) Triton X-100, and two times in PBS. Finally, the polyester membranes with the Caco-2 monolayers were excised from the Transwells and mounted on to slides using mounting medium (ProLong Gold Antifade Mountant with DAPI; Thermo Fisher Scientific, Waltham, USA).

Two fields of view were imaged for 11 of the 12 monolayers, as one of the monolayers was deemed unsuitable for imaging. Imaging of monolayers was performed on a Zeiss LSM 900 Airyscan 2 microscope in confocal mode using a 40 × NA 1.3 objective lens and a zoom of 1.00. Settings were kept constant across samples during acquisition. At 0.5 μm intervals, probes were excited with 488 nm and 568 nm laser light, and emitted photons were collected at 488–575 nm and 561–650 nm respectively. Cell nuclei (DAPI) were imaged with 405 nm excitation and 405–599 nm wavelengths. The amount of occludin and ZO-1 localised at the cell boundaries was quantified using Fiji/ImageJ (version 1.54f, open source software, GitHub) (Schindelin et al., 2012). Multichannel images were split into individual channels for analysis. To determine background fluorescence, z-series spanning the complete monolayer thickness were mean projected. Mean intensity was measured for each channel in 5 locations corresponding to cytoplasmic periphery and the nucleus using a circle region of interest of 5.02 μm diameter. Each averaged value was subtracted from its original single channel z-stack to create background corrected stacks. These were thresholded using the method of Otsu with the centre-most plane as

reference. Total fluorescence was measured using the Analyse Particles function with size exclusion set to 1.0 μm. Intensity was normalised against the total number of cells in a given field of view.

2.4. Transepithelial electrical resistance (TEER) assay

Transwell inserts with differentiated Caco-2 monolayers were transferred into cellZscope cell modules (nanoAnalytics, Munster, Germany), with each well containing 810 μL of MEM containing 10 % (v/v) FBS and 1 % (v/v) NEAA, and the baseline TEER was monitored overnight using a cellZscope controller (nanoAnalytics, Munster, Germnay) and software (version 4.3.1; nanoAnalytics, Munster, Germany). Caco-2 monolayers were then pre-treated with 0 or 1 mg·mL^{-1} whey, following which TEER was measured every hour for 24 h, after which point the treatment was removed and the cells were challenged. For studies on immune-mediated barrier dysfunction, the medium in the well was replaced with the equivalent medium containing 0–150 ng·mL^{-1} TNFa. For studies on the effects of intracellular ROS, the media in both the well and Transwell insert were replaced with their respective medium containing 0 or 1000 μM AAPH (Sigma-Aldrich, St. Louis, USA). Following the challenge, TEER was measured every hour for a further 48 h. For each timepoint, the percentage change in TEER was calculated using the following formula: change in TEER (%) = TEER (Ω.cm^2)/TEER$_0$ (Ω.cm^2) × 100–100 (%), where TEER$_0$ is the final baseline TEER value prior to pre-treatment. Only Caco-2 monolayers where both TEER$_0$ and TEER at the 1-h timepoint was >500 Ω.cm^{2}Ω cm^2 were considered for analysis, as a low initial TEER value suggests that the integrity of the monolayer was compromised prior to addition of the treatment. Monolayers where TEER dropped below 30 % of the baseline were also excluded from analysis.

2.5. Determination of intracellular reactive oxygen species generation

Intracellular ROS generation in Caco-2 cells was evaluated by intracellular oxidation of 2′,7′-dichlorofluorescin (DCFH) to the fluorescent compound 2′,7′-dichlorofluorescein (DFC) based on the method described by Wan et al. (Wan, Liu, Yu, Sun, & Li, 2015). The chemical 2′,7′-dichlorofluorescin diacetate (DCFH-DA) is able to cross the membrane of intact cells, following which it is hydrolysed by intracellular esterases to non-fluorescent DCFH (H. Wang & Joseph, 1999). However, in the presence of ROS, DCFH is oxidised to fluorescent DCF, enabling relative quantification of intracellular ROS by analysing DCF fluorescence.

Caco-2 cells were seeded on black 96-well plates (Corning, New York, USA) at a density of 5 × 10^4 cells/well and cultured for 24 h prior to treating cells with whey protein (0–1 mg·mL^{-1}) for a further 24 h. The treatment was then removed, and cells were incubated with 60 μM DCFH-DA (Sigma-Aldrich, St. Louis, USA) for 20 min. Following removal of DCFH-DA treatment, and washing of cells with PBS to remove unincorporated DCFH-DA, cells were challenged with AAPH (0–1000 μM) prepared in Hanks' Balanced Salt Solution (with calcium, magnesium, no phenol red; Thermo Fisher Scientific, Waltham, USA) containing 10 mM N-2-hydroxyethylpiperazine-N-2-ethane sulfonic acid (Thermo Fisher Scientific, Waltham, USA). The challenge medium was prepared both in the presence (0.1–1 mg·mL^{-1}) and absence of whey protein. Upon completion of the challenge (90 min), the level of intracellular ROS was determined by measuring the intensity of fluorescence at an excitation wavelength of 485 nm, and an emission wavelength of 538 nm using a plate reader (FlexStation 3, Molecular Devices, San Jose, USA). For each run of the experiment, fluorescence levels were normalised by dividing by the average value for control (untreated and unchallenged) samples.

2.6. Preparation of cells for proteomics analysis following oxidative stress

Caco-2 cells were seeded on tissue-culture-treated 6-well plates (Corning, New York, USA) at a density of 2.3 × 10^5 cells/well. Following 21 days of growth, Caco-2 monolayers were pretreated with 0 or 1 mg·mL^{-1} of whey (2.5 mL/well) for 24 h before removing the treatment and challenging the cells with 0 or 1000 μM AAPH (2.5 mL/well) for 90 min. The monolayers were then washed three times in cold PBS before lysing the cells in cold RIPA Lysis and Extraction Buffer (Thermo Fisher Scientific, Waltham, USA) supplemented with Roche cOmplete protease inhibitor cocktail (500 μL/well; Sigma-Aldrich, St. Louis, USA). Following a 25-min incubation on ice to ensure sufficient lysis, cell lysates were collected and stored at −80 °C until analysis.

2.7. Protein extraction

After the sample tubes were thawed, they were vortexed and placed on ice for further processing. The samples underwent two 5-s sonication rounds, with a 5-min interval on ice, using a 1/8" probe at 20 kHz with a 40 % amplitude of 40W (Vibra Cell™, Sonics&Matrials, Newtown, US). The lysed cells were rested on ice for 5 min before a final centrifugation for 15 min at 14,000×*g* at 4 °C to pellet the debris. The supernatant was transferred to new LoBind Eppendorf tubes and stored at −80 °C until further processing.

The supernatant was thawed on ice, centrifuged for 15 min at 20,000×*g* at 4 °C, and the protein concentration was determined with the detergent compatible Pierce 660 protein assay (Thermo, Waltham, USA). The samples were digested via an adjusted filter aided sample preparation (Wiśniewski, Zougman, Nagaraj, & Mann, 2009). In short, a volume equivalent to 50 μg total protein (27.5 μL) was pipetted into a NanoSep 10kD filter (Pall, New York, USA). The proteins were denatured in 100 μL urea (8 M, pH 8.0) and reduced with 20 μL dithiothreitol (500 mM) for 1 h at RT, shaking at 400 rpm (Thermo-Shaker, Thermo, Waltham, USA). The denatured samples were centrifuged for 15 min at 14,000×*g* at 20 °C until dry and washed three times with 300 μL urea (8M, pH 8.0). The reduced cysteines were alkylated through incubation with 2 μL 2-iodoacetamide (25 mM) in the dark for 1 h at RT, shaking at 400 rpm (Thermo-Shaker). After centrifugation for 15 min at 14,000×*g* at 20 °C, the samples were washed twice with 300 μL urea (8M, pH 8.0) and three times with 300 μL ammonium bicarbonate (50 mM). Next, the proteins were digested overnight at 37 °C with 3 μg trypsin (Promega, Leiden, Netherlands) in 100 μL ammonium bicarbonate (50 mM). The filters were centrifuged for 5 min at 14,000×*g* at 20 °C until dry. The filters were then washed with 100 μL ammonium bicarbonate (50 mM) and the eluates were collected in the same tube. The eluates were dried in a vacuum centrifuge. The pellet was rinsed with 250 μL of LC-MS grade water and dried again in a vacuum centrifuge. The peptide residual was stored at −80 °C until analysis.

2.8. Mass spectrometric data acquisition and protein identification

The dried eluates were resuspended in 50 μL 0.1 % formic acid and further diluted to obtain 0.1 μg·μL^{-1}. The samples were analysed by liquid chromatography mass spectrometry (LC-MS). For that, 2 μL of the sample solution (i.e. 200 ng) was injected on a nano-LC system (nanoElute, Bruker, Bremen, Germany), equipped with a reversed-phase C18 separation column (0.075 × 250 mm, 1.6 μm particle size, Aurora, Ionoptics, Melbourne, Australia). LC separation was performed at 50 °C with a flow rate of 0.3 μL ·min^{-1} and a mobile phase of solvent A (0.1 % formic acid in water) and solvent B (0.1 % formic acid in acetonitrile). The gradient was set as follows: 0 min, 2 % B; 90 min, 25 % B; 100 min, 50 % B; 100.5 min, 95 % B; and 109 min, 95 % B. Online MS measurements were performed on a trapped ion mobility spectrometry quadrupole time-of-flight mass spectrometer with a CaptiveSpray ionization source (ESI-TIMS-QqToF, timsTOF Pro 2, Bruker Daltonik, Bremen, Germany) in the positive ion mode. The source-drying temperature was set to 180 °C with a gas flow of 3 L ·min^{-1} and capillary voltage at 1500 V. Singly charged precursor and background ions were excluded from the polygon filter in m/z and mobility dimension. MS spectra were acquired within a 100–1700 m/z and 0.6 to 1.6 1/K0 (20 eV–59 eV

collision) mobility range, with an acquisition rate of 9.4 Hz. Ions within a mass range of 400–1200 Da and mobility range of 0.6–1.43 1/K0 were acquired using 32 consecutive data-independent acquisition parallel accumulation–serial fragmentation (DIA-PASEF) windows in a cycle time of 1.8 s.

Protein identification was performed in DIA-NN v1.8.1 (Demichev, Messner, Vernardis, Lilley, & Ralser, 2020) with a combined FASTA file comprised of the (reviewed + unreviewed) non-redundant Uniprot human database ID9606, downloaded October 10, 2022 (n = 145,142 human protein sequences) and the bovine milk proteome database BoMiProt 2.0 (Das, Giri, Behera, Maity, & Ambatipudi, 2022) (n = 10, 314 bovine milk protein sequences). The following parameters were used: FASTA digest and deep learning enabled, trypsin (–cut K*,R*,! R*P), 1 missed cleavage, max. 4 variable PTMs per peptide, fixed modification Carbamidomethylation, peptide length: 7–30, precursor charge: 1–4+, precursor range: 300–1800 m/z, fragment ion range: 200–1800 m/z, precursor FDR: 1 %, individual mass accuracy, unrelated runs, heuristic protein inference, neural network classifier: single pass mode, quantification: robust LC, cross-run normalisation: RT-dependent, library generation: smart profiling. All bovine annotated proteins (n = 446) were removed from the DIA-NN result output file prior to data analysis.

2.9. Statistical analysis

Statistical analysis and visualisations were performed and generated using R v4.3.1 (R Core Team, 2023), and the packages ggplot2 v3.4.2 (Wickham, 2016), pheatmap v1.0.12, VennDiagram v1.7.3., mixOmics v6.24.0, diann v1.0.1 and DEP v1.22.0. For TJ protein quantification, normalised fluorescence intensity measurements were fitted using a mixed model with treatment + challenge + treatment × challenge as fixed effects, and slide (monolayer) as a random effect. The effect of treatment on change in TEER over time was compared using a mixed-model analysis as the same monolayers were measured over time. Models were fitted by the restricted maximum-likelihood (REML) method using the nlme package v3.1 (Pinheiro, Bates, DebRoy, Sarkar, & R Core Team, 2024). The statistical model included the effect of treatment + time + treatment × time as fixed effects, and the Transwell inserts nested within blocks (where one run of an experiment was considered a block) as a random effect. If the treatment × time interaction was significant ($P < 0.05$), pairwise comparisons were applied using estimated marginal means using the emmeans package v1.8.8 (Lenth, 2024). The false discovery rate (q) was applied to the tests of the marginal means, with differences considered significant when $q < 0.05$. For intracellular ROS analysis, normalised fluorescence measurements were fitted using a linear model with treatment + block as fixed effects, where treatment was the treatment-challenge combination, and one run of an experiment was considered a block. Estimated marginal means and their confidence intervals were calculated using the emmeans package. Proteins identified by DIA-NN were filtered for a 1 % false discovery rate, prior to using MaxLFQ for calculating the protein abundance levels. After Quality control, the proteins were filtered to only include proteins measured in at least 60 % of the samples within each treatment group. Proteins tested for differential expression based on protein-wise linear models and empirical Bayes statistics using limma, as implemented by DEP (v1.22.0), and considered differentially expressed at an adjusted $P < 0.05$. Imputation of missing values was performed using the MinProb algorithm, as implemented in the R-package MSNbase. An upset plot was created with SubcellularVis (Watson, Smith, Francavilla, & Schwartz, 2022). GO and KEGG pathway enrichment analyses were conducted using the clusterProfiler package (version 4.10.0). The GO enrichment analysis included the assessment of the biological process (BP), cellular component (CC), and molecular function (MF). The GO and KEGG pathway enrichment analyses used Benjamini-Hochberg to set an adjusted significance threshold of $P < 0.05$.

3. Results

3.1. Effect of whey on localisation and abundance of tight junction proteins occludin and zona occludens-1 (ZO-1)

We used confocal microscopy to visualise the effects of whey on TJ protein abundance and localisation in Caco-2 monolayers that were concurrently challenged or unchallenged with TNFa for 24 h (Fig. 1a). For all four treatment-challenge combinations tested, both occludin and ZO-1 were localised at the cell boundaries, with little indication of protein internalisation. Fluorescence intensity at the cell boundaries was quantified out to determine relative protein abundance. For both occludin (Fig. 1b) and ZO-1 (Fig. 1c), the TNFa challenge appeared to reduce the TJ abundance for both whey treated and untreated monolayers. However, neither the treatment, challenge, nor treatment × challenge effects were significant ($P > 0.05$), indicating the abundance of TJ protein localised at the cell boundaries was not different between the four treatment-challenge groups in our experiment.

3.2. Effect of pre-treatment with whey on inflammation induced barrier dysfunction

Because functional foods such as whey protein supplements would usually be consumed as a prophylactic to prevent against inflammation or stress-induced barrier dysfunction, we sought to investigate whether pre-treatment with whey was sufficient to mitigate inflammation induced barrier dysfunction. To this end, we treated Caco-2 monolayers for 24 h (the 'pre-treatment period') with whey, following which the treatment was removed, and the monolayers were challenged with various concentrations of TNFa. We monitored the TEER across the monolayers in the 24 h prior to and 48 h following the challenge (Fig. 2). The time × treatment effect was significant ($P < 0.001$), so comparisons between treatment groups were performed.

In Caco-2 monolayers that were not pre-treated with whey, the TEER dropped by 38–40 % of $TEER_0$ in the 48 h following challenge, indicating a loss of barrier function (Fig. 2). In contrast, untreated-unchallenged monolayers only showed a drop of 7 % during the same period.

Compared to the untreated-unchallenged monolayers, the TEER in untreated monolayers challenged with 50 or 100 ng·mL^{-1} TNFa was significantly lower ($q < 0.05$) between the timepoints of 32–72 h. When challenged with 150 ng·mL^{-1} TNFa, the lower TEER could be observed slightly earlier (between 30 and 72 h). There were no other TEER differences between untreated monolayers challenged with 50, 100, or 150 ng ·mL^{-1} TNFa, indicating that there was no dose-effect of TNFa from 50 ng·mL^{-1} onwards.

In unchallenged monolayers (i.e., 0 ng·mL^{-1} TNFa), TEER increased ($q < 0.05$) in samples pre-treated with whey compared to untreated samples from 15 h following the addition of whey (Fig. 2). An increase in TEER was also observed for the TNFa-challenged groups (this effect was statistically significant in the 100 and 150 ng·mL^{-1} TNFa challenge groups). Pre-treated samples also showed a higher TEER compared to untreated samples during the pre-treatment period in the 100 and 150 ng/m ng·mL^{-1} L TNFa challenge groups. However, following the removal of whey at the 24-h timepoint, there was no difference in TEER between the pre-treated and untreated samples ($q > 0.05$ for all timepoints in the unchallenged group). This suggests that the whey must be present in the culture medium to exert its barrier enhancing properties.

Interestingly, following challenge with 50 ng·mL^{-1} TNFa, samples that were pre-treated with whey showed a greater drop in TEER than those that were not pre-treated (Fig. 2). However, this the effect was not present following challenge with 100 or 150 ng·mL^{-1} TNFa indicating that whey pre-treatment is not detrimental to barrier integrity during inflammation. Overall, despite whey previously being shown to mitigate TNFa mediated barrier dysfunction when present in the sample during challenge, the data indicates that pre-treatment with whey alone is not

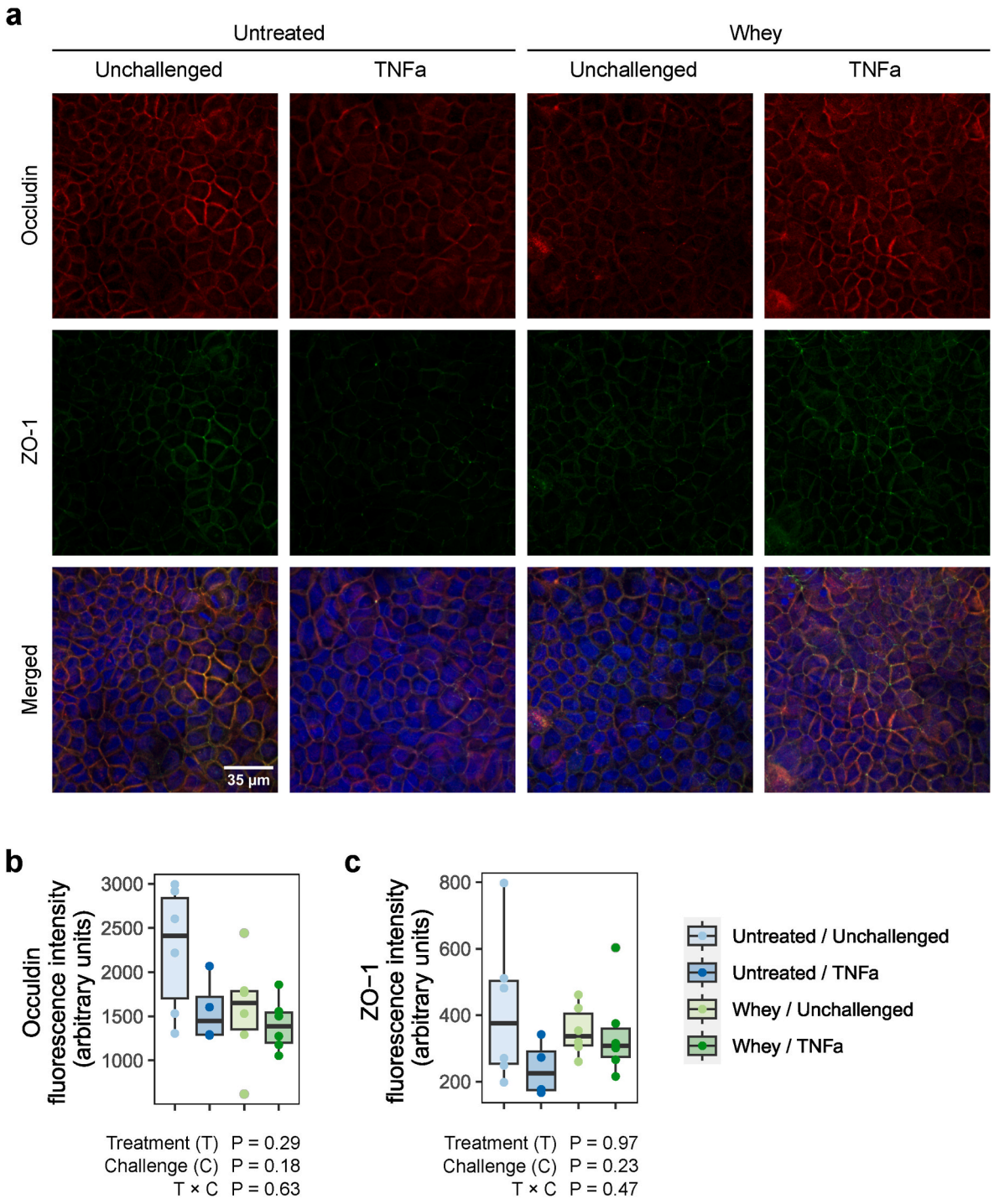

Fig. 1. Effect of whey treatment on immunolocalisation of occludin and zona occludens-1 (ZO-1) in Caco-2 monolayers challenged with TNFa. (a) Representative summed projections from z-series of Caco-2 monolayers treated with 1 mg·mL^{-1} whey, or left untreated for 24 h, and stained for occludin (red), ZO-1 (green), and DNA (blue). Untreated and whey-treated monolayers were either concurrently challenged with 100 ng·mL^{-1} TNFa, or left unchallenged. Scalebar, 35 µm. (b) Immunofluorescence analysis of occludin, and (c) ZO-1 localised at the cell boundaries (n = 4–6 fields of view per treatment). Box and whisker plots indicate the median (middle line), first and third quartile (boundaries of box), and 1.5 times the interquartile range (whiskers). The overlayed dots indicate the individual values. (For interpretation of the references to colour in this figure legend, the reader is referred to the Web version of this article.)

sufficient to protect against barrier dysfunction.

3.3. Effect of whey on oxidative stress in intestinal cells

Caco-2 cells were pretreated with various concentrations of whey, following which the cells were challenged with AAPH as a generator of peroxyl radicals (Bayram, Pekmez, Arda, & Yalçın, 2008; Corrochano, Buckin, Kelly, & Giblin, 2018). We examined the effect of AAPH on intracellular ROS under conditions where the whey treatment was removed prior to AAPH challenge (pre-treated only; Fig. 3a), as well as when the whey was added in during AAPH challenge (pre- and co-treated; Fig. 3b).

In the absence of pre-treatment with whey, the AAPH challenge resulted in a dose-dependent increase in intracellular ROS (Fig. 3a).

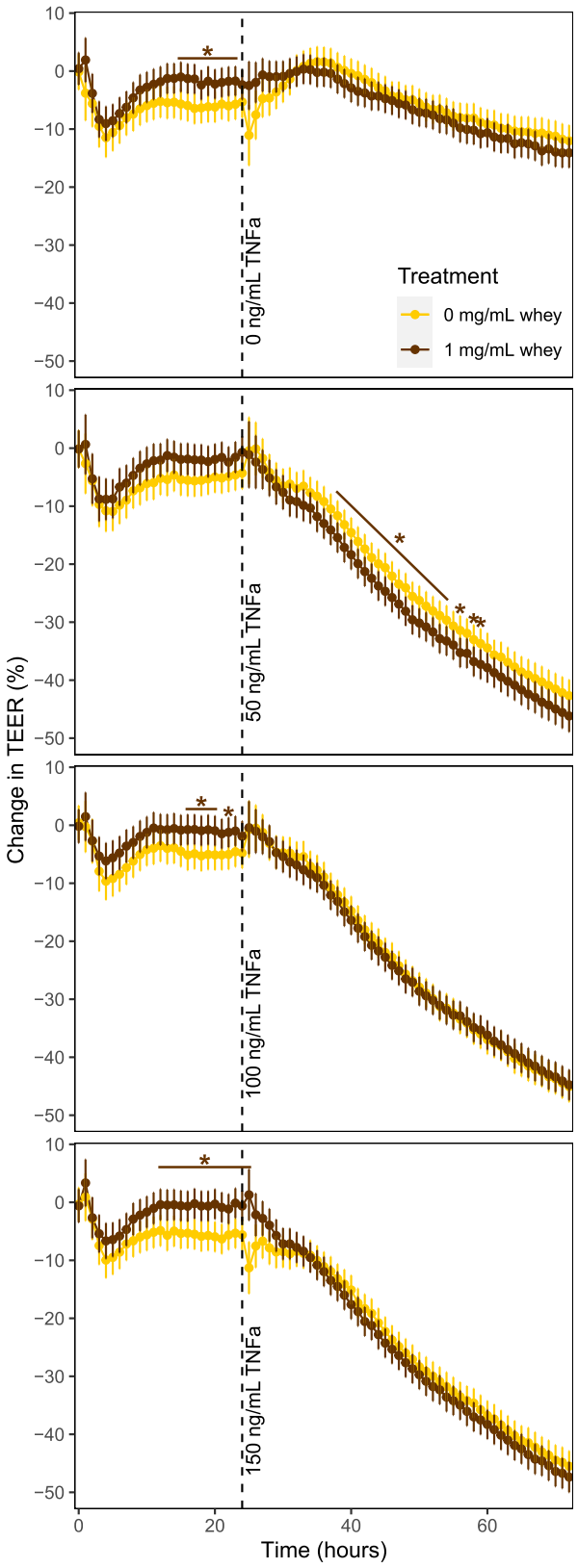

Fig. 2. Effect of pre-treatment with whey on the transepithelial electrical resistance (TEER) across Caco-2 monolayers challenged with TNFa. Caco-2 monolayers were treated with 0 or 1 mg·mL^{-1} whey for 24 h, following which the treatment medium was removed, and the cells were challenged with TNFa at the indicated concentration. Graph shows the estimated marginal mean (±SE) of the change in TEER over time (n = 11–13; 4 experiments; 2–5 samples per treatment per experiment). *q < 0.05 compared to 0 mg·mL^{-1} whey treatment.

However, when samples were pre-treated with whey, the levels of intracellular ROS dropped, again in a dose-dependent manner. Pre-treatment with whey at 0.5 mg·mL^{-1} was sufficient to prevent AAPH-mediated increase in intracellular ROS (up to 1000 μM AAPH).

Interestingly, when samples were pre-treated and co-treated with whey, treatment at 0.1 mg·mL^{-1} of whey exacerbated the AAPH induced increase in intracellular ROS (Fig. 3b). However, as the whey concentration was increased, the intracellular ROS levels showed a dose-dependent decrease. Pre- and co-treatment with 1 mg·mL^{-1} whey was sufficient to reduce intracellular ROS to baseline (control) levels.

As oxidative stress can lead to intestinal barrier dysfunction and disruption of TJ (Lambert et al., 2002; Rao, 2008), we hypothesised that pre-treatment of differentiated Caco-2 monolayers with whey would protect against AAPH-mediated barrier dysfunction. Unexpectedly, AAPH challenge resulted in an increase in TEER, and there was no statistical difference between samples that were (1 mg·mL^{-1}) and were not (0 mg·mL^{-1}) pre-treated (Fig. 3c).

3.4. *Intracellular proteome analysis via data-independent acquisition mass spectrometry*

Next, we employed untargeted mass spectrometry to gain a better understanding of how pre-treatment with whey mitigates the increase in intracellular ROS following AAPH-challenge by a comprehensive analysis of the intracellular proteome of Caco-2 cells. The proteome of the four treatment conditions was measured by data-independent acquisition mass spectrometry: (i) control (untreated unchallenged) cells (n = 3), (ii) untreated challenged cells (n = 5), (iii) pre-treated unchallenged cells (n = 3), and (iv) pre-treated challenged cells (n = 5). In a preliminary database search, multiple residual bovine whey proteins were identified in the samples after whey treatment. We therefore searched the data with a database that contained both bovine milk and human proteins and removed all identified bovine proteins (n = 446) from the results.

A total of 7128 non-redundant human proteins were identified in the whole dataset. The majority of the identified proteins localised to the cytoplasm and nucleus (Fig. 4a). Additional cellular compartments included the plasma membrane, cytoskeleton, golgi apparatus, and endoplasmic reticulum, which indicates full lysis and digestion of the epithelial cells. Prior to imputation, the data were filtered for <40 % missing values per condition, across multiple conditions, resulting in a reduced dataset of 7050 proteins. To ensure that on/off signals across the treatment groups were still captured for proteins, protein values were set to 0 in a treatment group if a protein is detected in less than 40 % of the samples per treatment group. Over 97 % (n = 6861) of the proteins were detected under all four conditions (Fig. 4b).

After imputation, principle component analysis (PCA) was used to explore how similar (or dissimilar) the protein profiles were across samples and to indicate the main sources of variance in the data (Fig. 4c). The first two components (PC1, PC2) collectively accounted for 49 % of the variance in the data, but did not effectively segregate the groups (Fig. 4c). The control (untreated-unchallenged) samples exhibited lower variation than the other three treatment conditions. This suggests that the dominant source of variation is likely biological in nature. Hence, further noise reduction within the dataset was essential to identify proteins with significant biological relevance and enable effective group differentiation. Next, a two-way hierarchical clustering method was applied, where samples and proteins are grouped according to their protein abundance profiles; and this clustering was applied independently to the columns and to the rows (Fig. 4d).

To further explore how well the (multivariate) subsets of proteins separated the four treatment conditions, supervised data reduction

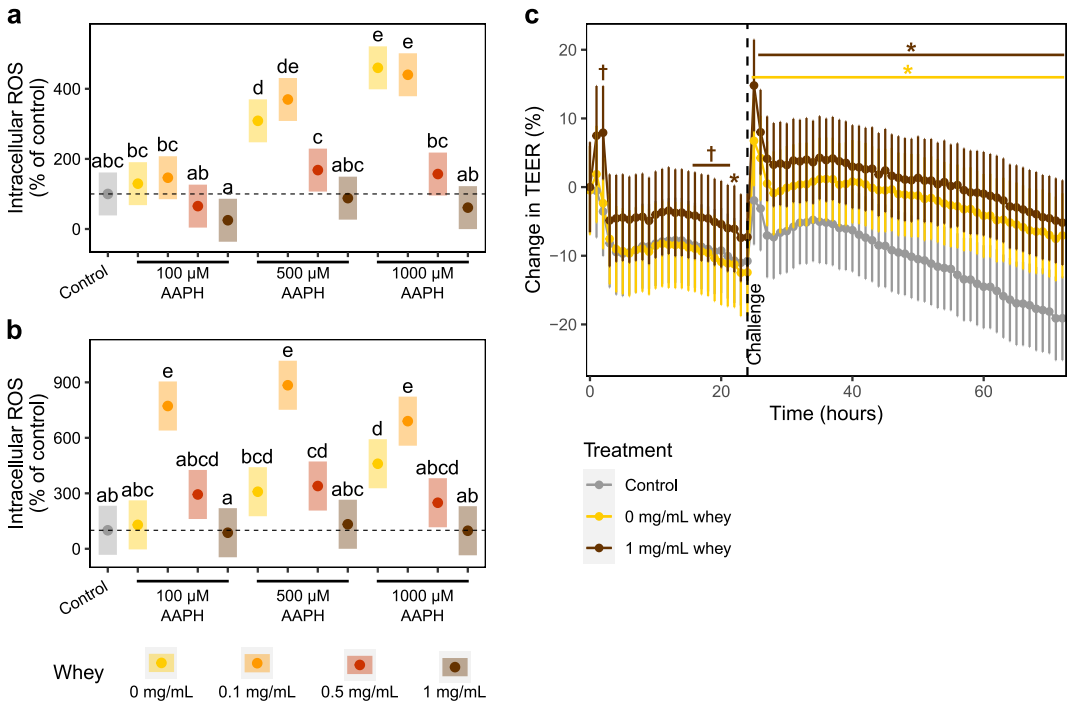

Fig. 3. Effect of whey treatment on Caco-2 cells following stimulation of oxidative stress. (a) Effect of 2,2′-Azobis (2-amidinopropane) dihydrochloride (AAPH) on generation of intracellular reactive oxygen species (ROS) in Caco-2 cells pre-treated with whey. Caco-2 cells were treated with whey at the indicated concentration for 24 h, following which the treatment was removed and the cells were challenged with the indicated concentration of AAPH for 90 min. Control cells were neither treated not challenged. Graph shows the estimated marginal means and 95 % confidence intervals (n = 12; 3 experiments, 4 samples per treatment per experiment). (b) Effect of AAPH on generation of ROS in Caco-2 cells pre-treated and co-treated with whey. Caco-2 cells were treated with whey at the indicated concentration for 24 h, following which cells were challenged with the indicated concentration AAPH, along with the whey treatment, for 90 min. Treatment groups that do not share the same letter are significantly different ($P < 0.05$). (c) Effect of pre-treatment with whey on the transepithelial electrical resistance (TEER) across Caco-2 monolayers challenged with AAPH. Caco-2 monolayers were treated with 0 or 1 mg·mL^{-1} whey for 24 h, following which the treatment medium was removed, and the cells were challenged with 1 mM AAPH. Control cells were neither treated nor challenged. Graph shows estimated marginal mean (±SE) of the change in TEER across time (n = 17–21; 2 experiments; 8–11 samples per treatment per experiment). $^{\dagger}q < 0.1$, $^{*}q < 0.05$ compared to control.

through a partial least square - discriminant analysis (PLS-DA) was performed on all proteins (n = 7050) (Fig. 5). The first latent variable (LV1) accounted for 36 % of the variance in the data and discriminated the untreated unchallenged cells mostly from the other three conditions, (Fig. 5a). LV2 (10 %) fully separated the untreated challenged cells from the other three treatment conditions. LV3 (7 %) predominantly separated the pre-treated unchallenged cells from the other three conditions (Fig. 5b). The plot showed that pre-treated challenged samples clustered more closely with untreated unchallenged samples than the other two treatment conditions.

To assess whether any proteins were present at different levels of abundance between the different treatment groups, protein abundance values were compared between the groups by fitting protein wise linear models and empirical Bayes statistics using limma, followed by Benjamini-Hochberg error correction on the p-values. In total 325 differentially expressed proteins (DEPs) were found to be significantly different between treatment groups. A full list is available in Table S 1.

Of particular interest in this work are TJ proteins. While TJ proteins ZO-3, ZO-1, and ZO-2, were identified and relatively quantified within the dataset, no significant difference between all treatment groups could be detected, though a trend of lower abundance in the untreated unchallenged group compared to the other three treatment groups was seen (Fig. 6). Junctional adhesion molecule A and occludin were identified and relatively quantified, but no significant changes in abundance were observed across treatment groups. In the claudin family of transmembrane tissue proteins, however, both claudin-1 and claudin-3 were identified to be significantly different between the untreated unchallenged vs pre-treated challenged treatment groups (Fig. 6), while claudin-4 and claudin-7 were not significantly different, though trends in abundances across groups are similar.

3.5. Pathway enrichment analysis

Gene Ontology (GO) and Kyoto Encyclopedia of Genes and Genomes (KEGG) pathway enrichment analysis of all DEPs was performed across the different treatment conditions to elucidate the biological roles of the DEPs. KEGG analysis indicated an enrichment in pathways linked to cytoskeleton in muscle cells and motor proteins across multiple comparisons, i.e. pre-treated unchallenged cells vs pre-treated challenged cells; untreated challenged cells vs pre-treated unchallenged cells and untreated unchallenged cells vs pre-treated unchallenged cells, indicating the relevance of these pathways in either whey-pretreatment or AAPH challenge of the cells (Figure S 1). The pairwise comparison of untreated challenged cells vs pre-treated unchallenged cells also showed an enrichment in complement and coagulation cascade pathway. All other pairwise comparison did not deliver any significantly enriched KEGG pathways.

To help understand the impact of whey pre-treatment on Caco-2 cells, further pairwise GO analysis was performed comparing the untreated unchallenged cells vs pre-treated unchallenged cells. In total 205 proteins were differentially abundant between the two treatments, with 151 protein more abundant in the pre-treated unchallenged samples and 54 proteins more abundant in the untreated unchallenged (control) samples. While no enriched GO-terms could be found to gain insights in the proteins more abundant the pre-treated unchallenged samples, several GO-terms were enriched for the proteins with higher abundance in the control (untreated unchallenged) samples. GO functional annotation revealed that these DEP were mainly associated with myofibril

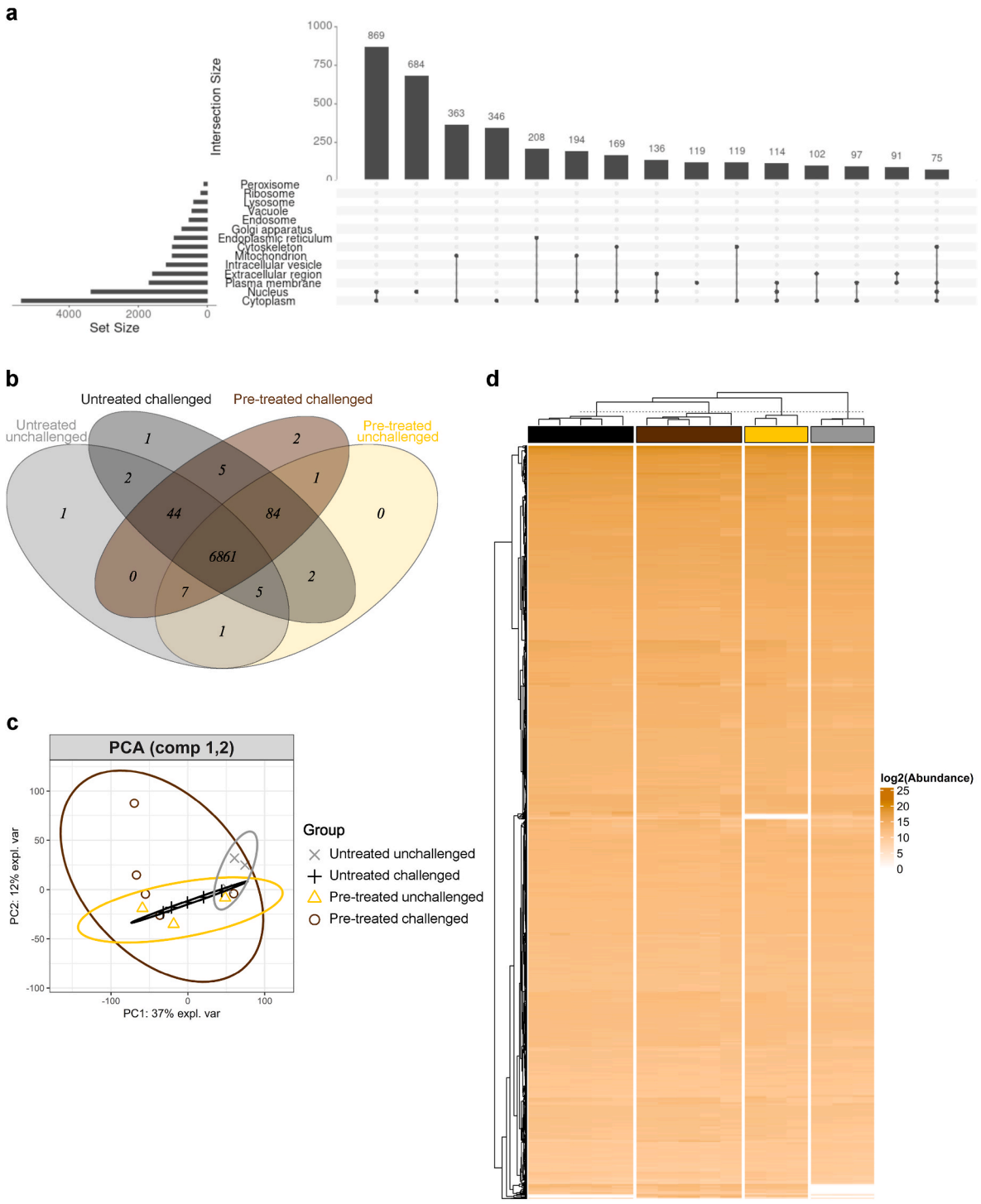

Fig. 4. Overview of the identified proteins in the dataset via a) Protein localisation upset plot (showing the first 15 out of 109 intersections), b) a VENN diagram comparing overlapping identified proteins between the four different experimental conditions, c) principle component analysis (PCA), showing the first two components accounting for 37 % and 12 % of the total variance, depicting individual samples including 95 % probability ellipses for each group, d) hierarchical clustering heatmap of all differentially expressed proteins (rows) and individual samples (columns) with a colour gradient representing the protein abundance. (For interpretation of the references to colour in this figure legend, the reader is referred to the Web version of this article.)

and muscle myosin complex cellular components (CC), muscle system binding and muscle contraction biological processes (BP), and actin filament and cytoskeletal motor activity as molecular function (MF) (Fig. 7). This indicates that whey-pretreatment might induce changes in the actin cytoskeleton network of the TJs.

3.6. Lasting effect of whey pre-treatment on the intestinal epithelial intercellular proteome

Next, we investigated which of the whey pre-treatment induced protein abundance differences remained following the AAPH challenge, to elucidate mechanisms underlying adaptative cell responses. Whey pre-treatment caused a lasting effect on 27 proteins (Table S 2), i.e.

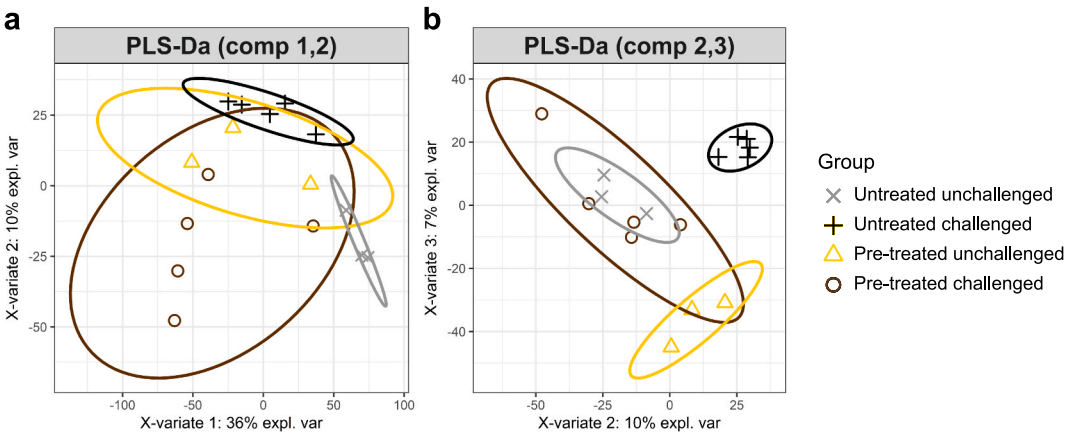

Fig. 5. Partial least-square discriminant analysis (PLS-DA) on <40 % imputation filtered proteins (n = 7050) illustrates the reduced dimensions of the dataset, by combining the optimal subset of proteins that best describe the variance between the different conditions in decreasing order, showing the individual samples per condition including a 95 % probability ellipse for a) latent variable 1 and 2 (46 % of total variation), and b) latent variable 2 and 3 (17 % of total variation).

protein levels of pre-treated challenged cells and pre-treated unchallenged cells were similar to each other, but significantly different from the untreated challenged cells. Not surprisingly, most of the proteins were absent in the control (untreated unchallenged) group and/or untreated challenged group, indicating most likely a specific expression upon pre-treatment with whey, which was maintained after AAPH challenge. Of note were MICAL-like protein 1, a protein linked to the regulation of establishment of TJs, as well as an extracellular matrix-associated protein(fibulin-1), and a protein associated with the epithelial-mesenchymal transition (epsin-3) (Fig. 8), both of which have been linked to loss of intercellular adhesion (Ichikawa-Tomikawa, Sugimoto, Satohisa, Nishiura, & Chiba, 2011).

Additionally, some proteins, such as fibrinogen alpha, which is associated with re-epithelisation, showed a significant decrease in abundance after whey pre-treatment, which was retained after the challenge (Fig. 8). A similar trend for the beta and gamma subunit of fibrinogen supports this finding. Inversely, transcriptional regulation factor 1 protein levels displayed a significant increase in abundance in untreated challenged cells compared to untreated unchallenged cells, however there was no difference between untreated unchallenged and the two pre-treated treatment conditions (Fig. 8).

4. Discussion

In this study we investigated the effects of a commercially available whey protein ingredient (all whey proteins in bovine milk with a pI > 6.8) on intestinal epithelial function where Caco-2 cells were challenged with an inflammatory (TNFa) or oxidative-stress (AAPH) mediator. While it was previously shown that TNFa-mediated reduction in TEER can be mitigated by 1 mg·mL^{-1} whey when the treatment is present during the TNFa challenge (Ulluwishewa et al., 2022), the effect of pre-treatment was unknown. In the current study, it was demonstrated that pre-treatment with 1 mg·mL^{-1} whey was not able to mitigate the TNFa-induced barrier dysfunction. However, consistent with our hypothesis, pre-treatment of Caco-2 cells with whey was able to reduce the production of AAPH-induced intracellular ROS, indicating that whey protein does not need to be present during the oxidative stress challenge to exert its antioxidative properties.

Prior to exerting their bioactive properties on the intestinal epithelium, ingested proteins would first undergo digestion in gastrointestinal tract (Giromini et al., 2019). Hence a major limitation of the present study was that the epithelial cells were treated with whey in its undigested form. Enzymatic hydrolysis of whey proteins by digestive enzymes in combination with fermentation or proteolysis by microbial or plant derived enzymes is known to modify their bioactivity (Korhonen, 2010). A study comparing bovine whey protein isolate (WPI) before and after simulated gastrointestinal digestion showed that the antioxidant activity of WPI increased following digestion (Corrochano et al., 2019). Hence to understand the full bioactive capacity of the whey ingredient used in this study, the effects of the ingredient in its digested form should also be investigated. Nonetheless, this study provides information regarding the potential synergistic properties of the protein milieu in the whey ingredient, which can aid in the understanding of its barrier enhancing and protective mechanisms.

As whey protein has previously been shown to mitigate TNFa-induced loss-of barrier function, we first investigated whether whey exerted this effect on Caco-2 monolayers via the modulation of abundance and localisation of TJ proteins. TNFa-mediated loss-of-TEER has in part been attributed to the downregulation and altered localisation of the ZO-1 TJ protein (Ma et al., 2004). Similarly, increases in intestinal permeability induced by TNFa have been shown to result from the downregulation of the TJ protein occludin (Li et al., 2012). However, in our experiments, while occludin and ZO-1 appeared to reduce in abundance under TNFa challenge, this effect could not be overcome by concurrent whey protein treatment. Whey protein treatment in the absence of challenge also showed no effect on occludin and ZO-1 localisation. Interestingly, bovine lactoferrin at 100 μg·mL^{-1} has previously shown to increase protein expression of occludin and ZO-1 in Caco-2 monolayers (Zhao et al., 2019), indicating that the mechanisms by which whey protein acts on these cells is different to that of lactoferrin on its own. Overall, the data suggest that the protective effects of whey against TNFa-mediated barrier dysfunction are unlikely to be due to the prevention of downregulation and re-localisation of these TJ proteins.

To determine whether anti-inflammatory benefits of whey pre-treatment were dependent on the level of inflammatory stress, TNFa challenge was introduced at a range of concentrations (0, 50, 100, and 150 ng·mL^{-1}). However, there were no TEER differences between untreated monolayers challenged with 50, 100, or 150 ng·mL^{-1} TNFa, indicating no dose-effect of TNFa from 50 mg·mL^{-1} onwards. This observation was consistent with previous reports where the highest effect of TNFa on TEER could be observed when challenged at 10 ng·mL^{-1} (Ma et al., 2004; Schnur et al., 2022). Samples were pre-treated with 1 mg·mL^{-1} whey because this concentration was previously shown to mitigate TNFa-induced loss of TEER when whey was present in the culture medium during challenge (Ulluwishewa et al., 2022). However, in the present study, pre-treatment with 1 mg·mL^{-1} whey did not mitigate the loss of TEER caused by any of the concentrations of TNFa tested.

Bovine whey proteins are known to exhibit antioxidative properties

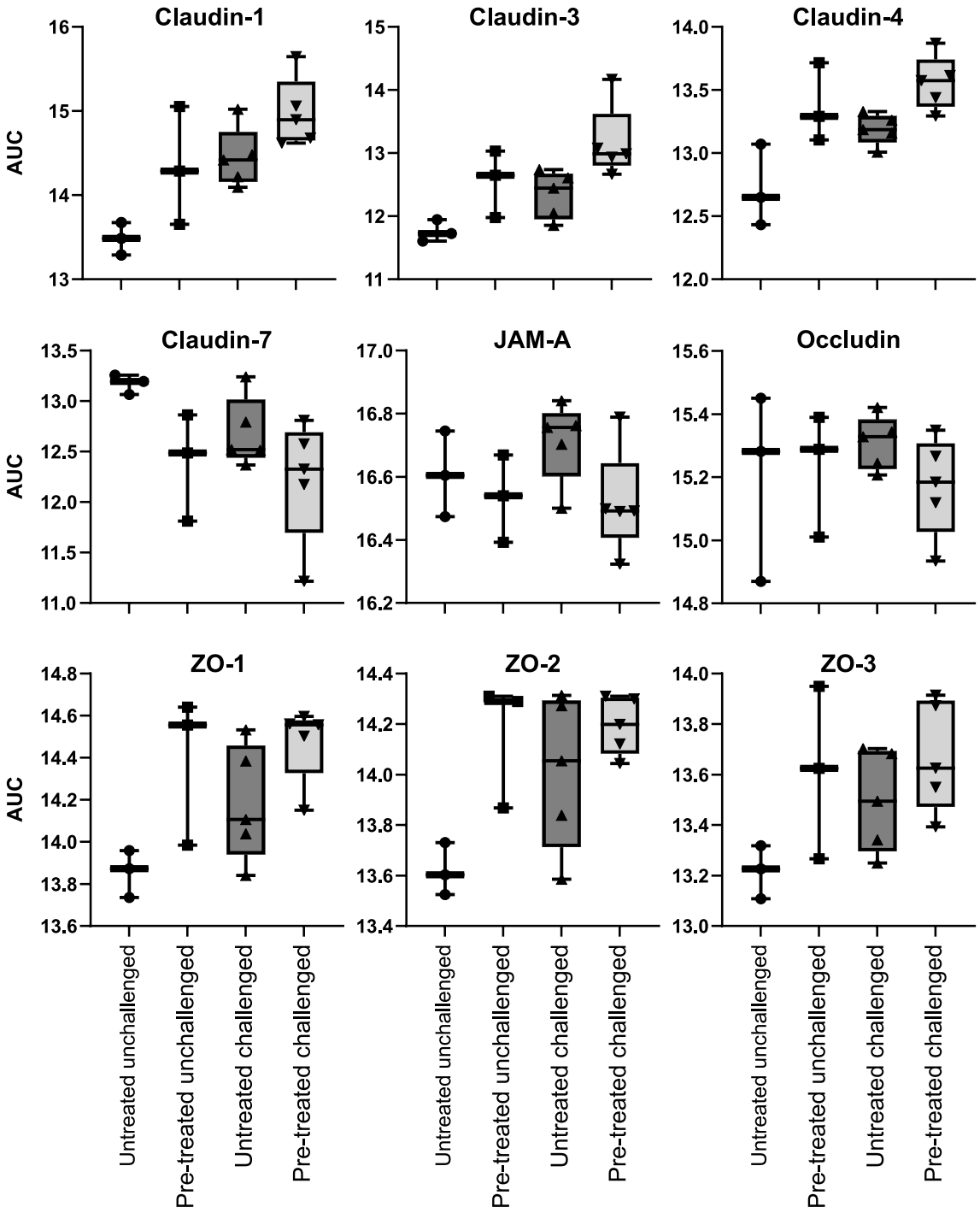

Fig. 6. Effect of whey pre-treatment tight junction protein abundance in Caco-2 cells challenged (or not) with 2,2′-azobis (2-amidinopropane) dihydrochloride (AAPH). Box and whiskers plots illustrate the abundance (area under the curve, AUC) of the identified major tight junction proteins across the four treatment conditions. Each data point represents an individual biological replicate. The boundaries of the box extends from the 25th to 75th percentiles, and the horizontal line within the box indicates the median value, while the whiskers indicate the minimum and maximum values.

(Bayram et al., 2008; Corrochano et al., 2018), and the whey protein ingredient used in this study is marketed as antioxidative due to its relatively high Oxygen Radical Absorbance Capacity value of 25,500 μmol Trolox equivalent (TE)/100 g (Quantec limited., 2012). Our results indicate that pre-treatment of intestinal cells with whey reduces intracellular ROS following AAPH challenge. These antioxidative properties of whey maybe, at least partly, due to the presence of lactoferrin and lactoperoxidase, which have been shown to reduce oxidative stress in Caco-2 cells (Abad et al., 2022; Matsushita et al., 2008). Moreover, lactoperoxidase is known to catalyse a redox reaction where the ROS H_2O_2 is reduced to H_2O (Tenovuo, Pruitt, Mansson-Rahemtulla, Harrington, & Baldone, 1986). However, further research is required to understand the reason for the increase in ROS during co-treatment with low concentrations of whey. We speculate that the addition of whey may initially accelerate AAPH decomposition, resulting in a higher production of ROS (Werber, Wang, Milligan, Li, & Ji, 2011). However, as the concentration of whey increases, its antioxidant capacity may become dominant, thereby reducing oxidative stress. This is consistent with

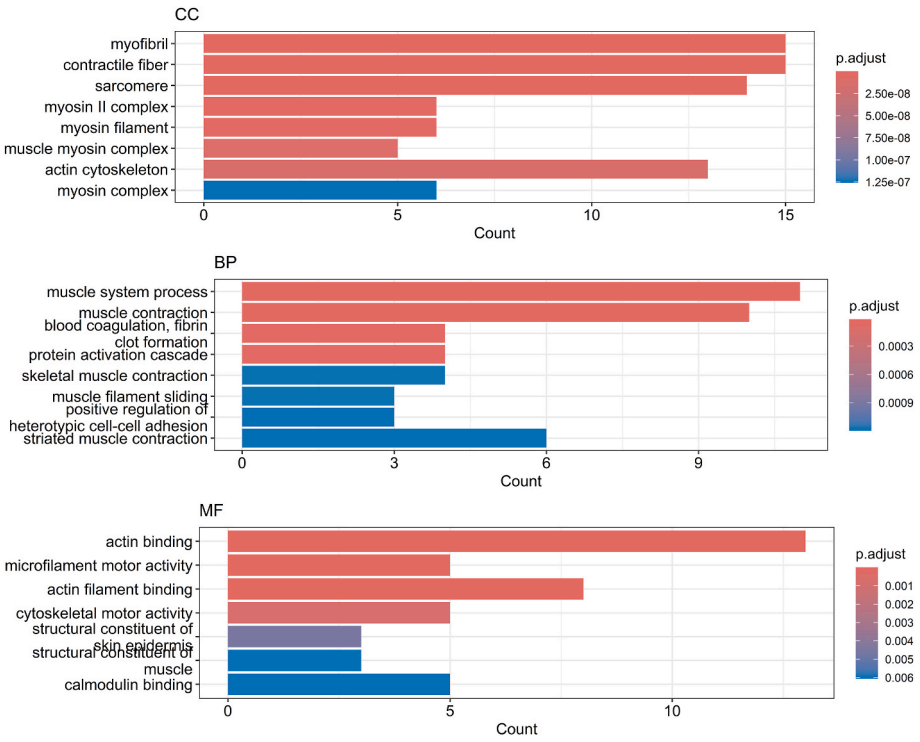

Fig. 7. Enriched Gene Ontology terms (cellular component (CC), biological process (BP), and molecular function (MF)) of differentially expressed proteins that are more abundant in control (untreated unchallenged) cells compared to pre-treated unchallenged cells.

lactoperoxidase, as with all heme peroxidases, being both a promoter and suppressor of ROS (Schaffer & Bronnikova, 2012).

Our data indicate that in the absence of challenge, whey treatment increases TEER in Caco-2 monolayers. This is consistent with a previous study (Ulluwishewa et al., 2022), and maybe due to individual proteins, or combinations of proteins present in the whey treatment. For example, a study by Zhao et al. showed that lactoferrin alone increases TEER across Caco-2 monolayers (Zhao et al., 2019), while a study by Anderson et al. showed that pure lactoferrin does not increase TEER, but that lactoferrin samples consisting of angiogenin does increase TEER (Anderson et al., 2017).

However, in contrast to previous studies that have shown that TEER decreases in Caco-2 monolayers in response to ROS generators, and that pre-treatment with ROS scavengers mitigate the oxidative-stress induced barrier dysfunction (Araki et al., 2005; Nallathambi, Poulev, Zuk, & Raskin, 2020), in our study AAPH did not decrease TEER across Caco-2 monolayers. However, only a limited number of studies have investigated the effects of AAPH on Caco-2 barrier function (Azzini et al., 2016; Gao et al., 2021). While these studies have demonstrated a reduction in TEER in response to AAPH challenge, one study did not disclose the concentration of AAPH used (Azzini et al., 2016), while the other study used AAPH at 20 mM (Gao et al., 2021) (20 × the concentration used in the present study). Neither provided details on whether the monolayers were challenged apically or basally. Thus, it may be possible to cause a decrease in TEER via modification of the challenge dose and protocol, following which the response may be modified by whey treatment.

To gain insights into how pre-treatment with whey mitigates the AAPH-induced increase in ROS, we measured the proteome of Caco-2 cells that were (or not) pre-treated with whey and/or challenged with AAPH. Of the 7050 proteins quantified in this experiment, 325 had significantly different abundances across the four treatment groups. While KEGG pathway enrichment analysis of DEPs across the treatment conditions revealed that the majority of the enriched pathways are associated with the cytoskeleton in muscle cells and motor proteins, and enriched GO terms were associated with similar processes such as muscle system process, actin filament binding and muscle contraction. The particular enrichment in actin regulation processes aligns with recent findings that indicate coupling of the actin cytoskeleton to adhesive membrane proteins at the TJ which helps to control the permeability of epithelial monolayers (Belardi et al., 2020). GO terms specifically related to cell-cell junction (GO:0005911), intestinal epithelial cell development (GO:0060,576), or response to oxidative stress (GO:0006979) were not significantly enriched in any condition.

While we could not directly link the DEPs to altered TJ function through GO pathway enrichment analysis, we observed a significant abundance increase of claudin-1 and claudin-3 TJ proteins in pre-treated and/or challenged cells. As claudins are known to play a central role in defining TEER and selectivity of the TJ barrier, these observations indicate mechanisms by which whey pre-treatment might enhance intestinal barrier function. Additionally, we observed a strong increasing trend for claudin-4, ZO-1, and ZO-2 TJ proteins in response to AAPH challenge as well as whey pre-treatment (Fig. 6). However, the variability within each treatment likely limited the significance of the observed effects in our current study. This is consistent with the observed increase in TEER in AAPH-challenged monolayers in this study, as previous studies have shown that expression of claudin-1 and -4 is associated with increased barrier function and TEER, although claudin-3 has been shown to have no effect on TEER (Günzel & Yu, 2013; Vreeburg, van Wezel, Ocaña-Calahorro, & Mes, 2012). ZO-1 and -2 are similarly associated with increased epithelial integrity (Cario, Gerken, & Podolsky, 2004; Ma et al., 2004). Interestingly, although some variation with the current sample set is seen, most of the whey pretreated samples demonstrated a higher abundance of ZO-1 compared to untreated samples, which could indicate the initiation of re-localisation of ZO-1. However, junctional adhesion molecules (JAMs) and occludin, which are also important in maintaining epithelial barrier integrity (Balda et al., 1996; Liu et al., 2000) showed no difference between the treatment conditions, suggesting these proteins were not involved in the change in TEER caused by whey or AAPH. Specific

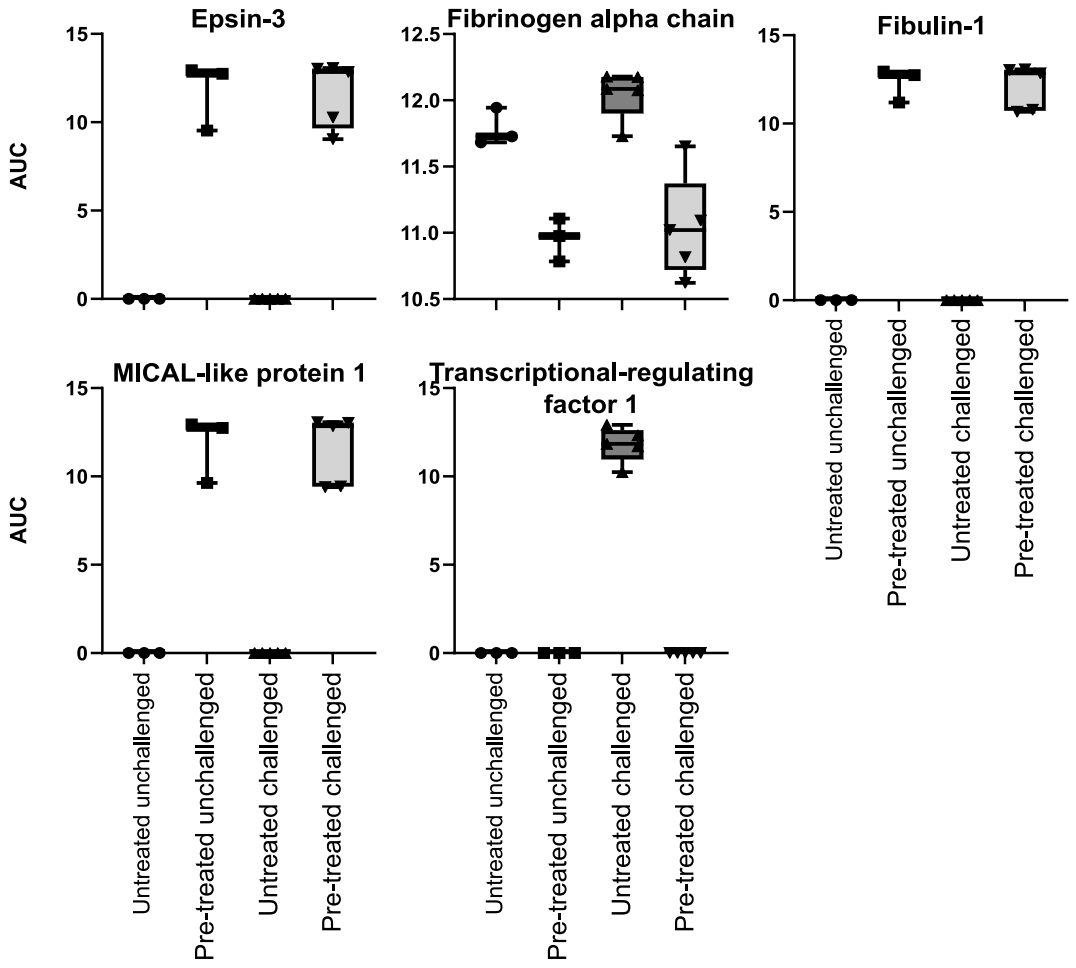

Fig. 8. Examples of lasting effects after whey treatment on protein levels. Box and whisker plots illustrate the abundance (area under the curve, AUC) of proteins across the four treatment conditions. Each data point represents an individual biological replicate. The boundaries of the box extends from the 25th to 75th percentiles, and the horizontal line within the box indicates the median value, while the whiskers indicate the minimum and maximum values.

proteins involved in the mechanisms on regulating oxidative stress response weren't detected, indicating that the AAPH challenge might not have been extreme enough to observe additional differences at a proteome level. Of the 27 proteins where the effect of whey pre-treatment persisted following the AAPH challenge, the majority were involved in transcriptional regulation, cell response, extracellular matrix or membrane rearrangements indicating major involvement in actin cytoskeletal rearrangements.

The aim of the proteomics study was to gain an unbiased overview of the Caco-2 proteome in response to oxidative stress and/or whey as an initial exploration. Although we found several highly potential candidates associated with the intestinal barrier function response, further research is required to confirm our findings. Kinetic studies through targeted analysis, such as parallel reaction monitoring mass spectrometry or immunoassays, would enable the quantification of proteins of interest and further elucidation of involved pathways. However, protein abundance levels alone are often insufficient for a comprehensive understanding of cellular processes. To delve deeper into underlying mechanisms, redox proteomics (Yang, Carroll, & Liebler, 2016) could be used to explore ROS induced modifications, such as phosphorylation (especially in MAPK pathway activation) (Rezatabar et al., 2019), ubiquitination (Stankovic-Valentin & Melchior, 2018), and glycosylation (Taniguchi et al., 2016). For instance, fibrinogen, which is a significant marker in this dataset, is considered one of the most vulnerable targets for oxidant attack (Kaufmanova et al., 2021). Further investigation into changes in its numerous disulfide bonds, phosphorylation sites, and glycosylation sites during oxidative stress might contribute to a deeper understanding of its role in the cellular response to oxidative stress and how whey might regulate its expression and function.

5. Conclusions

Whey containing all bovine milk whey proteins with pI > 6.8, in approximately the same ratio as found natively in bovine milk, can mitigate the production of intracellular ROS in intestinal epithelial cells *in vitro*. This anti-oxidative effect of whey is apparent even in cells where the whey treatment is removed prior to the addition of the pro-oxidative AAPH challenge. Similarly, proteomic analysis showed that whey has a lasting effect on the expression levels on a small subset of cellular proteins even after the challenge. In contrast, while whey increased intestinal barrier function as measured by TEER, this beneficial effect was transient, with TEER returning to the level of untreated control monolayers following removal of the whey treatment. These data suggest that whey may be consumed as prophylactic against the effects of oxidative stress in the gastrointestinal tract. The presence of whey in the digesta may enhance intestinal barrier function, while the antioxidative effects likely continue even after the whey transits through the gastrointestinal tract. However, it should be noted that when consumed, gastrointestinal digestion of whey may modify its bioactivity which could lead to an altered cellular response.

Immunohistochemistry studies indicated that the whey-induced improvement in barrier function was unlikely to be due to the abundance and localisation of the occludin or ZO-1 TJ proteins, while proteomics studies indicated involvement of the claudin-1 and -3 TJ

proteins, and cytoskeletal rearrangement in the AAPH and whey induced increase in TEER. As the antioxidative effects of whey persisted following removal of pre-treatment, it indicates an adaptation of the cells in response to the whey pre-treatment and/or that the proteins were bound or internalised by the cells allowing them to exert their effects following removal of the treatment. However further research is required to confirm the mechanisms via which whey exerts its barrier-enhancing and antioxidative properties. An in-depth understanding of these mechanisms, as well the key components in whey responsible for the observed properties, can help accelerate the development of dairy-derived supplements that serve as natural antioxidants and help maintain proper intestinal function.

CRediT authorship contribution statement

Esther Willems: Writing – original draft, Methodology, Investigation, Formal analysis. **Ajitpal Purba:** Methodology, Investigation. **Matthew S. Savoian:** Methodology, Formal analysis. **Charles Hefer:** Visualization, Formal analysis. **Evelyne Maes:** Writing – review & editing, Writing – original draft, Supervision, Formal analysis. **Dulantha Ulluwishewa:** Writing – review & editing, Writing – original draft, Visualization, Funding acquisition, Formal analysis, Conceptualization.

Declaration of competing interest

The authors declare the following financial interests/personal relationships which may be considered as potential competing interests: The study was co-funded by Quantec Ltd. Quantec Ltd. manages the manufacture of and markets and exports the whey protein ingredient used in this study.

Acknowledgements

This study was funded by the Ministry of Business, Innovation and Employment (Wellington, New Zealand) through the High-Value Nutrition National Science Challenge (Auckland, New Zealand) Contestable Fund (contract HVN 1940), and through the Strategic Science Investment Fund (AgResearch contract: A25977: Systems Biology Enabling Platform), and Quantec Ltd (Hamilton, New Zealand). Imaging was performed at Manawatu Microscopy & Imaging Centre (Palmerston North, New Zealand). The authors are grateful to Dr Harold Henderson (AgResearch Ruakura Research Centre) for statistical advice.

Appendix A. Supplementary data

Supplementary data to this article can be found online at https://doi.org/10.1016/j.idairyj.2025.106187.

References

Abad, I., Sangüesa, A., Ubieto, M., Carramiñana, J. J., Pérez, M. D., Buey, B., et al. (2022). Protective effect of bovine lactoferrin against Cronobacter sakazakii in human intestinal Caco-2/TC7 cells. *International Dairy Journal, 133*, Article 105428.

Abd El-Salam, M. H., & El-Shibiny, S. (2017). Separation of bioactive whey proteins and peptides. In *Ingredients extraction by physicochemical methods in food* (pp. 463–494).

Anderson, R. C., Bassett, S. A., Haggarty, N. W., Gopal, P. K., Armstrong, K. M., & Roy, N. C. (2017). Short communication: Early-lactation, but not mid-lactation, bovine lactoferrin preparation increases epithelial barrier integrity of Caco-2 cell layers. *Journal of Dairy Science, 100*, 886–891.

Araki, Y., Katoh, T., Ogawa, A., Bamba, S., Andoh, A., Koyama, S., et al. (2005). Bile acid modulates transepithelial permeability via the generation of reactive oxygen species in the Caco-2 cell line. *Free Radical Biology and Medicine, 39*, 769–780.

Azzini, E., Maiani, G., Garaguso, I., Polito, A., Foddai, M. S., Venneria, E., et al. (2016). The potential health benefits of polyphenol-rich extracts from cichorium intybus L. Studied on caco-2 cells model. *Oxidative Medicine and Cellular Longevity, 2016*, Article 1594616.

Balda, M. S., Whitney, J. A., Flores, C., Gonzalez, S., Cereijido, M., & Matter, K. (1996). Functional dissociation of paracellular permeability and transepithelial electrical resistance and disruption of the apical-basolateral intramembrane diffusion barrier by expression of a mutant tight junction membrane protein. *Journal of Cell Biology, 134*, 1031–1049.

Basuroy, S., Sheth, P., Kuppuswamy, D., Balasubramanian, S., Ray, R. M., & Rao, R. K. (2003). Expression of kinase-inactive c-src delays oxidative stress-induced disassembly and accelerates calcium-mediated reassembly of tight junctions in the caco-2 cell monolayer. *Journal of Biological Chemistry, 278*, 11916–11924.

Bayram, T., Pekmez, M., Arda, N., & Yalçın, A. S. (2008). Antioxidant activity of whey protein fractions isolated by gel exclusion chromatography and protease treatment. *Talanta, 75*, 705–709.

Belardi, B., Hamkins-Indik, T., Harris, A. R., Kim, J., Xu, K., & Fletcher, D. A. (2020). A weak link with actin organizes tight junctions to control epithelial permeability. *Developmental Cell, 54*, 792–804. e797.

Bischoff, S. C., Barbara, G., Buurman, W., Ockhuizen, T., Schulzke, J. D., Serino, M., et al. (2014). Intestinal permeability–a new target for disease prevention and therapy. *BMC Gastroenterology, 14*, 189.

Cario, E., Gerken, G., & Podolsky, D. K. (2004). Toll-like receptor 2 enhances ZO-1-associated intestinal epithelial barrier integrity via protein kinase C. *Gastroenterology, 127*, 224–238.

Corrochano, A. R., Buckin, V., Kelly, P. M., & Giblin, L. (2018). Invited review: Whey proteins as antioxidants and promoters of cellular antioxidant pathways. *Journal of Dairy Science, 101*, 4747–4761.

Corrochano, A. R., Saricay, Y., Arranz, E., Kelly, P. M., Buckin, V., & Giblin, L. (2019). Comparison of antioxidant activities of bovine whey proteins before and after simulated gastrointestinal digestion. *Journal of Dairy Science, 102*, 54–67.

Das, A., Giri, K., Behera, R. N., Maity, S., & Ambatipudi, K. (2022). BoMiProt 2.0: An update of the bovine milk protein database. *Journal of Proteomics, 267*, Article 104696.

Demichev, V., Messner, C. B., Vernardis, S. I., Lilley, K. S., & Ralser, M. (2020). DIA-NN: Neural networks and interference correction enable deep proteome coverage in high throughput. *Nature Methods, 17*, 41–44.

Farnaud, S., & Evans, R. W. (2003). Lactoferrin—a multifunctional protein with antimicrobial properties. *Molecular Immunology, 40*, 395–405.

Günzel, D., & Yu, A. S. L. (2013). Claudins and the modulation of tight junction permeability. *Physiological Reviews, 93*, 525–569.

Gao, G., Zhou, J., Jin, Y., Wang, H., Ding, Y., Zhou, J., et al. (2021). Nanoparticles derived from porcine bone soup attenuate oxidative stress-induced intestinal barrier injury in Caco-2 cell monolayer model. *Journal of Functional Foods, 83*.

Giromini, C., Cheli, F., Rebucci, R., & Baldi, A. (2019). Invited review: Dairy proteins and bioactive peptides: Modeling digestion and the intestinal barrier. *Journal of Dairy Science, 102*, 929–942.

Graikini, D., García, L., Abad, I., Lavilla, M., Puértolas, E., Pérez, M. D., et al. (2024). Antirotaviral activity of dairy byproducts enriched in fractions from hyperimmune bovine colostrum: The effect of thermal and high hydrostatic pressure treatments. *Food & Function, 15*, 2265–2281.

Hidalgo, I. J., Raub, T. J., & Borchardt, R. T. (1989). Characterization of the human colon carcinoma cell line (Caco-2) as a model system for intestinal epithelial permeability. *Gastroenterology, 96*, 736–749.

Ichikawa-Tomikawa, N., Sugimoto, K., Satohisa, S., Nishiura, K., & Chiba, H. (2011). Possible involvement of tight junctions, extracellular matrix and nuclear receptors in epithelial differentiation. *Journal of Biomedicine and Biotechnology, 2011*, Article 253048.

Kaufmanova, J., Stikarova, J., Hlavackova, A., Chrastinova, L., Maly, M., Suttnar, J., et al. (2021). Fibrin clot formation under oxidative stress conditions. *Antioxidants, 10*.

Korhonen, H. J. (2010). Health-promoting proteins and peptides in colostrum and whey. In Y. Mine, E. Li-Chan, & B. Jiang (Eds.), *Bioactive proteins and peptides as functional foods and nutraceuticals* (pp. 149–168). Oxford, UK: Wiley-Blackwell.

Lambert, G. P., Gisolfi, C. V., Berg, D. J., Moseley, P. L., Oberley, L. W., & Kregel, K. C. (2002). Selected contribution: Hyperthermia-induced intestinal permeability and the role of oxidative and nitrosative stress. *Journal of Applied Physiology, 92*, 1750–1761. ; discussion 1749.

Lenth, R. V. (2024). emmeans: Estimated marginal means, aka least-squares means_. *R package version 1.8.7*. https://CRAN.R-project.org/package=emmeans.

Li, G. Z., Wang, Z. H., Cui, W., Fu, J. L., Wang, Y. R., & Liu, P. (2012). Tumor necrosis factor alpha increases intestinal permeability in mice with fulminant hepatic failure. *World Journal of Gastroenterology, 18*, 5042–5050.

Liu, Y., Nusrat, A., Schnell, F. J., Reaves, T. A., Walsh, S., Pochet, M., et al. (2000). Human junction adhesion molecule regulates tight junction resealing in epithelia. *Journal of Cell Science, 113*(Pt 13), 2363–2374.

Ma, T. Y., Iwamoto, G. K., Hoa, N. T., Akotia, V., Pedram, A., Boivin, M. A., et al. (2004). TNF-alpha-induced increase in intestinal epithelial tight junction permeability requires NF-kappa B activation. *American Journal of Physiology - Gastrointestinal and Liver Physiology, 286*, G367–G376.

Matsushita, A., Son, D. O., Satsu, H., Takano, Y., Kawakami, H., Totsuka, M., et al. (2008). Inhibitory effect of lactoperoxidase on the secretion of proinflammatory cytokine interleukin-8 in human intestinal epithelial Caco-2 cells. *International Dairy Journal, 18*, 932–938.

Nallathambi, R., Poulev, A., Zuk, J. B., & Raskin, I. (2020). Proanthocyanidin-rich grape seed extract reduces inflammation and oxidative stress and restores tight junction barrier function in caco-2 colon cells. *Nutrients, 12*.

Ostertag, F., & Hinrichs, J. (2023). Enrichment of lactoferrin and immunoglobulin G from acid whey by cross-flow filtration. *Foods, 12*, 2163.

Pinheiro, J., Bates, D., DebRoy, S., Sarkar, D., & R Core Team. (2024). nlme: Linear and nonlinear mixed effects models_. *R package version, 3*, 1–144. https://CRAN.R-project.org/package=nlme.

Pinto, M., Robine, S., & Appay, M. D. (1983). Enterocyte-like differentiation and polarization of the human colon carcinoma cell line CACO-2 in culture. *Biology of the Cell, 47*, 323–330.

Quantec limited. (2012). *Technical note 1.0 clinical studies summary on IDP® Hamilton, New Zealand: Quantec limited*.
R Core Team. (2023). *R: A language and environment for statistical computing*. Vienna, Austria: R Foundation for Statistical Computing. https://www.R-project.org/.
Rao, R. (2008). Oxidative stress-induced disruption of epithelial and endothelial tight junctions. *Frontiers in Bioscience, 13*, 7210–7226.
Rezatabar, S., Karimian, A., Rameshknia, V., Parsian, H., Majidinia, M., Kopi, T. A., et al. (2019). RAS/MAPK signaling functions in oxidative stress, DNA damage response and cancer progression. *Journal of Cellular Physiology, 234*, 14951–14965.
Samak, G., Gangwar, R., Meena, A. S., Rao, R. G., Shukla, P. K., Manda, B., et al. (2016). Calcium channels and oxidative stress mediate a synergistic disruption of tight junctions by ethanol and acetaldehyde in caco-2 cell monolayers. *Scientific Reports, 6*, Article 38899.
Schaffer, W. M., & Bronnikova, T. V. (2012). Peroxidase-ROS interactions. *Nonlinear Dynamics, 68*, 413–430.
Schindelin, J., Arganda-Carreras, I., Frise, E., Kaynig, V., Longair, M., Pietzsch, T., et al. (2012). Fiji: An open-source platform for biological-image analysis. *Nature Methods, 9*, 676–682.
Schnur, S., Wahl, V., Metz, J. K., Gillmann, J., Hans, F., Rotermund, K., et al. (2022). Inflammatory bowel disease addressed by caco-2 and monocyte-derived macrophages: An opportunity for an in vitro drug screening assay. *In Vitro Model, 1*, 365–383.
Stankovic-Valentin, N., & Melchior, F. (2018). Control of SUMO and ubiquitin by ROS: Signaling and disease implications. *Molecular Aspects of Medicine, 63*, 3–17.
Stolfi, C., Maresca, C., Monteleone, G., & Laudisi, F. (2022). Implication of intestinal barrier dysfunction in gut dysbiosis and diseases. *Biomedicines, 10*.
Suzuki, T. (2013). Regulation of intestinal epithelial permeability by tight junctions. *Cellular and Molecular Life Sciences, 70*, 631–659.
Taniguchi, N., Kizuka, Y., Takamatsu, S., Miyoshi, E., Gao, C., Suzuki, K., et al. (2016). Glyco-redox, a link between oxidative stress and changes of glycans: Lessons from research on glutathione, reactive oxygen and nitrogen species to glycobiology. *Archives of Biochemistry and Biophysics, 595*, 72–80.
Tenovuo, J., Pruitt, K. M., Mansson-Rahemtulla, B., Harrington, P., & Baldone, D. C. (1986). Products of thiocyanate peroxidation: Properties and reaction mechanisms. *Biochimica et Biophysica Acta (BBA) - Protein Structure and Molecular Enzymology, 870*, 377–384.
Ulluwishewa, D., Mullaney, J., Adam, K., Claycomb, R., & Anderson, R. C. (2022). A bioactive bovine whey protein extract improves intestinal barrier function in vitro. *JDS communications, 3*, 387–392.
Vreeburg, R. A., van Wezel, E. E., Ocaña-Calahorro, F., & Mes, J. J. (2012). Apple extract induces increased epithelial resistance and claudin 4 expression in Caco-2 cells. *Journal of the Science of Food and Agriculture, 92*, 439–444.
Wan, H., Liu, D., Yu, X., Sun, H., & Li, Y. (2015). A Caco-2 cell-based quantitative antioxidant activity assay for antioxidants. *Food Chemistry, 175*, 601–608.
Wang, Y., Chen, Y., Zhang, X., Lu, Y., & Chen, H. (2020). New insights in intestinal oxidative stress damage and the health intervention effects of nutrients: A review. *Journal of Functional Foods, 75*.
Wang, H., & Joseph, J. A. (1999). Quantifying cellular oxidative stress by dichlorofluorescein assay using microplate reader. *Free Radical Biology and Medicine, 27*, 612–616.
Watson, J., Smith, M., Francavilla, C., & Schwartz, J.-M. (2022). SubcellulaRVis: A web-based tool to simplify and visualise subcellular compartment enrichment. *Nucleic Acids Research, 50*, W718–W725.
Werber, J., Wang, Y. J., Milligan, M., Li, X., & Ji, J. A. (2011). Analysis of 2,2'-azobis (2-amidinopropane) dihydrochloride degradation and hydrolysis in aqueous solutions. *Journal of Pharmaceutical Sciences, 100*, 3307–3315.
Wiśniewski, J. R., Zougman, A., Nagaraj, N., & Mann, M. (2009). Universal sample preparation method for proteome analysis. *Nature Methods, 6*, 359–362.
Wickham, H. (2016). *ggplot2: Elegant graphics for data analysis. New York, NY*. New York: Springer-Verlag.
Yang, J., Carroll, K. S., & Liebler, D. C. (2016). The expanding landscape of the thiol redox proteome. *Molecular and Cellular Proteomics, 15*, 1–11.
Zhao, X., Xu, X. X., Liu, Y., Xi, E. Z., An, J. J., Tabys, D., et al. (2019). The in vitro protective role of bovine lactoferrin on intestinal epithelial barrier. *Molecules, 24*.